10-2-2020

Laboratory evaluation of the residue of rubber-modified emulsified asphalt

Dongdong Ge
Michigan Technological University, dge1@mtu.edu

Xiaodong Zhou
Michigan Technological University, xzhou3@mtu.edu

Siyu Chen
Michigan Technological University, siychen@mtu.edu

Dongzhao Jin
Michigan Technological University, dongj@mtu.edu

Zhanping You
Michigan Technological University, liyou@mtu.edu

sustainability

MDPI

Article

Laboratory Evaluation of the Residue of Rubber-Modified Emulsified Asphalt

Dongdong Ge, Xiaodong Zhou, Siyu Chen, Dongzhao Jin and Zhanping You *

Department of Civil and Environmental Engineering, Michigan Technological University, 1400 Townsend Drive, Houghton, MI 49931-1295, USA; dge1@mtu.edu (D.G.); xzhou3@mtu.edu (X.Z.); siychen@mtu.edu (S.C.); dongj@mtu.edu (D.J.)

* Correspondence: zyou@mtu.edu; Tel.: +1-906-487-1059

Received: 16 September 2020; Accepted: 9 October 2020; Published: 12 October 2020

Abstract: Emulsified asphalt has been widely used in various surface treatment methods such as chip seal for low-volume road preservation. Using modified emulsified asphalt made it possible to use chip seal technology on medium- and even high-volume traffic pavements. The main objective of the study is to quantify the residue characteristics of rubber-modified emulsified asphalt and to assess the effectiveness of using crumb rubber to modify emulsified asphalt binder. The four emulsified asphalt residues used the distillation procedure. Then, the rheology characteristics of emulsified asphalt residue were evaluated. The Fourier transform infrared spectroscopy (FTIR) test analyzed the chemical change of emulsified asphalt during the aging procedure. The results indicate that the evaporation method cannot remove all the water in emulsified asphalt. The mass change during the rolling thin film oven (RTFO) process only represented the component change of emulsified asphalt binder residue. Both the high-temperature and low-temperature performance grade of the two emulsified asphalt binders with rubber were lower. The original asphalt binder adopted to emulsification had a crucial influence on the performance of emulsified asphalt. The rubber modification enhanced the property of the emulsified asphalt binder at low temperatures, and the improvement effect was enhanced as the rubber content in the emulsified asphalt was raised. The C=O band was more effective in quantifying the aging condition of the residue. The findings of this study may further advance the emulsified asphalt technology in pavement construction and maintenance.

Keywords: emulsified asphalt; residue; binder performance; FTIR; aging

1. Introduction

Emulsified asphalt is produced by dispersing asphalt globules in water with surfactant and some other minor ingredients [1,2]. Emulsified asphalt is mainly used for low-volume pavement preservation, which includes chip seal, tack coat, and hot-in-place recycling [3]. Currently, more than 10% of asphalt in asphalt pavement is used in the form of emulsified asphalt [4]. Emulsified asphalt can effectively decrease asphalt viscosity at low temperatures. The energy depletion and carbon emissions during the production process can be significantly reduced when compared with the conventional hot mix asphalt mixture [5].

The application of emulsified asphalt in the chip seal was prominent for the preservation maintenance of low-volume pavement. The improvement of emulsion formulation made it possible to use chip seal technology on medium and high traffic conditions [6]. Modified asphalt emulsion with styrene-butadiene rubber and natural rubber could remarkably improve the stiffness of the emulsion residue and decrease the temperature sensitivity [7–10]. Tire rubber-modified asphalt emulsion had better aging resistance than the conventional and polymer-modified asphalt emulsion. The rheological and moisture stability of tire rubber-modified asphalt emulsion had comparable or

better performance [11]. The microstructure and the dispersion of the polymer in the emulsified asphalt could be evaluated with confocal microscopy, with the influence of different polymer addition methods being assessed. The distribution of polymer in the emulsified asphalt was more even than that in the hot polymer-modified asphalt [12]. The emulsion dispersion and property were also influenced by the binder resource [13]. The sieve test could be used to determine the oversized particle in emulsified asphalt, which evaluates the difficulty of emulsified asphalt application during the handling and application process. The particle size in emulsified asphalt was found to be influenced by storage, pumping, handling, and temperature [14]. The mechanical and thermal properties of emulsified asphalt were improved after polyurethane (PU) modification of the spatial molecular structure of the emulsified asphalt [15]. The settlement and storage stability test determined the differences between the percentage residue in the surface and the leveling layer of the emulsified asphalt in the storage container for a specified period [16]. Only a limited dosage of PU could be used to modify the emulsified asphalt since the storage stability of the emulsion will be weakened if the dosage of PU is too high [17]. The moisture sensitivity of asphalt emulsion with epoxy resin was found to be decreased, and the complex modulus, rutting, and fatigue properties of the asphalt emulsion residues were improved [18].

As a cost-effective and environmentally friendly strategy, more and more attention is being paid to cold recycling asphalt pavement. Using emulsified asphalt to produce cold recycled asphalt pavement with 100% reclaimed asphalt pavement (RAP) in the base layer of the pavement proved to be realistic to consume the RAP [19,20]. Due to the higher moisture susceptibility of the cold recycling mixture, the widespread application of cold recycling mixture was restricted. Among different factors, the aggregate coating was one of the most critical parameters [21]. The uniformity and film thickness of emulsified asphalt was influenced by the viscosity of emulsified asphalt. Emulsified asphalt with too high viscosity may block the spray bar, and thus the emulsified asphalt may not be applied evenly. On the other hand, emulsified asphalt with too low viscosity will easily flow away, thus influencing the quality of the emulsified asphalt application [22]. The effective surface area of the aggregate in the RAP was found to be decreased, and therefore sufficient new asphalt needs to be adopted to guarantee the coating property in the mixture [23]. The bond between emulsion and aggregate in the cold recycling mixture was found to be significantly influenced by the coating property, and the bond was fundamental in terms of guaranteeing the durability of the cold recycling mixture [24]. The adhesion between asphalt binder and fine aggregate could be improved by adding cement, thus increasing the moisture stability of the mixture with 100% RAP [25]. The cement could hydrate with the water residue in the emulsified asphalt and increase the bonding between the mastic and aggregate. The tensile strength, rutting, and moisture sensitivity of the mixture could be significantly improved by selecting optimum cement dosage [26]. The performance of the cold recycling mixture could also be enhanced by using modified asphalt emulsions. The polyvinyl acetate-modified asphalt emulsion could improve the compressive strength of the cold recycling mixture, thus increasing the rutting resistance of the mixture [27]. According to the cyclic creep test results, the polymer modification remarkably enhances the property of the cold recycling mixture [28].

The emulsified asphalt residue property reflects the performance of asphalt binder without water. Some researchers have proposed evaluation systems to quantify the emulsion residue characteristics, but limited values for different test parameters have been suggested [29]. The limitation criteria should be proposed for emulsified asphalt that is used under various regions and climate conditions, such as the emulsified asphalt used in the wet-freeze climate. The emulsified asphalt binder residue needs to be obtained before quantifying the grade of the emulsified asphalt. Currently, different recovery methods have been adopted to obtain emulsified asphalt binder residue by removing the water in emulsified asphalt. On the basis of the American Society for Testing and Materials (ASTM) D7497, low temperatures (25 °C and 60 °C) were adopted to recover residue from emulsified asphalt using the low-temperature evaporation method [30]. The two temperatures were chosen due to their similar temperatures to the field condition [31]. By conditioning emulsified asphalt at 60 °C for 6 h, the influence of aging on the residue was analyzed [32]. However, the recovery method that used low

and medium temperatures had the potential of water not being totally removed. The Karl Fischer (KF) titration method could be used to quantify the water in the emulsified asphalt residue [33]. In terms of the ASTM D6934, a certain weight of emulsified asphalt was placed in the baker and heated in the oven for 3 h at 163 °C [34]. In line with the ASTM D6997, emulsified asphalt was heated in an aluminum alloy to 260 °C for 15 min to acquire the emulsified asphalt residue [35]. The high temperature guaranteed that the water can be totally removed from the emulsified asphalt. Mitchell et al. adopted the hot oven procedure, stirred-can procedure, and warm oven method to obtain the residue. Size exclusion chromatography was applied to evaluate the existence of water, proving that there was no water residue in the recovered asphalt binder [36]. Salomon used distillation, evaporation, and moisture analyzer balance procedures to obtain the residue. The rheological property and the influence of aging during the recovery procedure of three residues were different [37]. The evaporation method also affected the rheological properties of residues [38]. Islam et al. assessed the influence of curing times, temperatures, and pressures on the property of the emulsified asphalt residue [39]. There is no agreement on the most effective recovery method or which method could represent the real asphalt residue in the field. Different methods may be needed for different types of modified emulsified asphalt. This paper will follow the ASTM D6934 and the ASTM D6997 to recover emulsified asphalt and assess the emulsified asphalt residue.

2. Motivations and Objectives

The paper is motivated by the application of ground tire rubber to modify emulsified asphalt. Using rubber-modified emulsified asphalt could relieve the influence of waste tire on the environment, which provided a cost-effective strategy to increase the adoption of rubber on the pavement.

The main objective of the study was to quantify the residue characteristics of rubber-modified emulsified asphalt and to assess the effectiveness of using crumb rubber to modify emulsified asphalt binder, thus extending the application of crumb rubber in the asphalt pavement. The property of emulsified asphalt with rubber was compared with that of the emulsified asphalt with polymer and conventional emulsified asphalt. The four emulsified asphalts used in wet-freeze climates were analyzed. The efficiency of the distillation and evaporation test procedure was assessed. The rheological property and the low-temperature property of emulsified asphalt residue were analyzed. The effect of aging on the emulsified asphalt residue was also discussed.

3. Materials and Methods

3.1. Materials

Four emulsified asphalts—CRS-2P, CSS-1H, CRS-2M, and CRS-2TR—were used in the study. CRS-2P is polymer-modified emulsified asphalt. CRS-2M is styrene-butadiene-styrene (SBS)-modified emulsified asphalt with 2% rubber. CRS-2TR is tire rubber-modified emulsified asphalt. The tire rubber content in CRS-2TR emulsified asphalt is 5%. CSS-1H is conventional emulsified asphalt. The technical performance of the four emulsified asphalt binders is displayed in Table 1. The test materials and test methods are displayed in Table 2.

Table 1. The technical properties of different emulsified asphalts.

Property	CRS-2P	CSS-1H	CRS-2M	CRS-2TR
Viscosity, SFS@50 °C, s	76	84	200	498.5
Residue by distillation, %	69.6	63.5	68.0	65.5
Demulsibility, %	76.8	-	74.6	47.8
Penetration, 100 g, 5 s, dmm, 25 °C	106	53	110	116
Ductility, 5 cm/min, cm, 25 °C	350	106	70	65
Sieve Test, %, wt	0.78	0	0.05	0

Table 2. Test materials and test methods.

Materials		**CRS-2P, CRS-2M, CSS-1H, and CRS-2TR**	
Test methods	DSR	Unaged and RTFO aged (34 to 82 °C, 6 °C increment)	Frequency (0.1, 1, 1.59, 3, 5, and 10 Hz)
		PAV aged (13 to 25 °C, 3 °C increment)	
	ABCD	Test temperature (10 °C to −60 °C)	
	FTIR	Wavelength (600–4000 cm^{-1}), resolution (4 cm^{-1})	

3.2. Test Methods

The distillation and evaporation methods were adopted to obtain CSS-1H residue. The efficiency of the two methods in removing water in emulsified asphalt was assessed. The more effective method, the distillation method, was used to obtain the residue of different emulsified asphalt binders. The performance of emulsified asphalt residue was assessed using different test methods. In order to guarantee the repeatability of the test results, we used at least three samples for each test.

a. Emulsified asphalt distillation

Emulsified asphalt binders were heated in an aluminum alloy still to 260 °C to obtain the emulsified asphalt residue by following ASTM D6997. The distilled emulsified asphalt residue was collected for further testing.

b. Residue obtain methods comparison

In order to compare the efficiency of the evaporation and distillation procedure in removing the water in emulsified asphalt residue, we conducted two procedures on the CSS-1H. The evaporation residue was collected by heating CSS-1H at 163 °C for 3 h to expel water in the emulsified asphalt, which followed the ASTM D6934 procedure.

c. Rolling thin film oven (RTFO)

The RTFO test was adopted to measure the influence of air and heat on the aging property of emulsified asphalt residue, according to the ASTM D2872. The moving film of emulsified asphalt residue was heated in an oven for 85 min at 163 °C [40]. The mass change of emulsified asphalt residue can be determined, which can reflect the volatility and the oxidation of the residue.

d. Pressure aging vessel (PAV)

The PAV test represented the accelerated aging of emulsified asphalt residue under compressed air and elevated temperature, which is consistent with the ASTM D6521. The RTFO-aged emulsified asphalt residue was aged at 100 °C for 20 h with 2.10 MPa air pressure [41].

e. Dynamic shear rheometer (DSR)

The DSR test was used to quantify the residue rheological property of emulsified asphalt. The complex shear modulus (|G*|) and phase angle (δ) of the sample are acquired with the DSR test [42]. The DSR temperature sweeps of unaged and RTFO-aged residues were conducted from 34 °C to 82 °C with a 6 °C increment. For the PAV-aged asphalt binder, we conducted the DSR temperature sweeps from 25 °C to 13 °C with a 3 °C decrement. Six frequencies (0.1, 1, 1.59, 3, 5, and 10 Hz) were adopted for every temperature sweep of residues experiencing the different aging procedure. The test parameters of the DSR test are displayed in Table 1.

f. Asphalt binder cracking device (ABCD)

The cracking temperature of emulsified asphalt residue was obtained by the ABCD test, and the test was followed by the AASHTO TP92. The fracture stress of the residue when cracking could directly reflect the low-temperature property of the residue [43]. The ABCD test can also assess the low-temperature property improvement because of modification [44,45]. The ABCD test was conducted on the ABCD test apparatus from EZ Asphalt Technology. The cracking temperature of emulsified asphalt residue was determined when strain jump occurred during the cooling process [46]. The fracture

stress was obtained on the basis of the strain jump from the test with Equation (1). Moreover, the low temperature of Performance Grading (PG) grade by ABCD was acquired on the basis of Equation (2).

$$\text{Fracture stress (MPa)} = (\text{Strain Jump, } \mu\varepsilon) \times 0.157 \quad (1)$$

$$\text{PG Grade by ABCD (°C)} = 0.78 \times (\text{ABCD cracking temp, °C}) - 0.9 \quad (2)$$

g. FTIR

The chemical interaction of emulsified asphalt residue could be validated with the FTIR test method [47]. The functional group could be adopted as an indicator to assess the asphalt modification effect [48,49]. The Jasco FT/IR 4200 FTIR spectrometer was used to quantify the chemical components of emulsified asphalt residue. The spectra wavelength ranged from 600 to 4000 cm^{-1} with a resolution of 4 cm^{-1}. For every sample, we used 64 scan times to guarantee the stability of the results, as displayed in Table 1. The –OH (3200–3550 cm^{-1}) functional group was selected for the CSS-1H residue with evaporation and distillation method to compare the efficiency of the two methods in removing the water in emulsified asphalt residue. The changing of C=O and S=O groups could be used to quantify the aging effect [50]. Bands near 1700 cm^{-1} were the stretch of C=O, and bands near 1000 cm^{-1} were the movement of S=O [51].

4. Test Results and Analysis

4.1. The Comparison of Evaporation and Distillation Procedure

The –OH (3200–3550 cm^{-1}) functional group was selected to validate the existence of water in residue obtained with the distillation and evaporation methods. The FTIR test results of two CSS-1H residues are shown in Figure 1. The CSS-1H residue after the evaporation procedure peaked during 3200–3550 cm^{-1}, which proved the existence of water in the residue. However, there was no peak during 3200–3550 cm^{-1} for CSS-1H after the distillation procedure. Using the evaporation method to obtain the emulsified asphalt residue cannot remove all the water in emulsified asphalt, thus influencing the property of emulsified asphalt residue. The characteristics evaluation of the emulsified asphalt of the following tests was conducted on residue acquired with the distillation method.

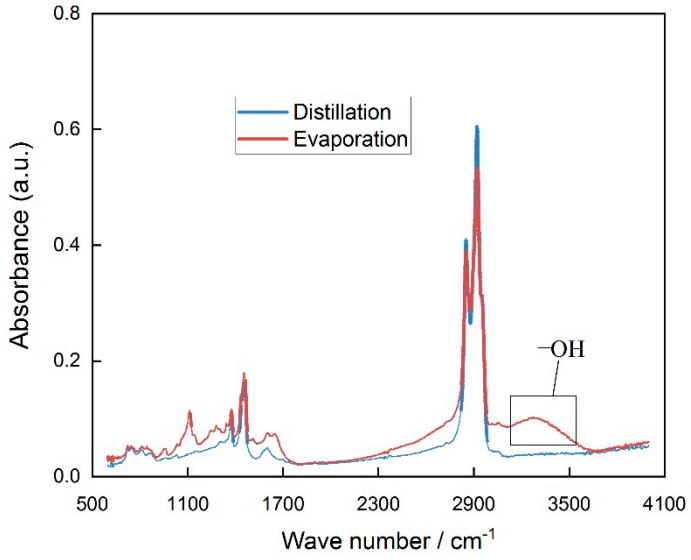

Figure 1. The FTIR of CSS-1H residue with the distillation and evaporation method.

4.2. The Mass Change during the RTFO Test

The evaporation of light compositions in residue reduced the mass, and the mass raised when it interacted with oxygen. The mass change during the RTFO process is due to the synthetic interaction of the volatilization and oxidation process. The mass change of four emulsified asphalt residues after the RTFO test is displayed in Figure 2. The standard deviation (SD) of the mass loss for the test results are also included in Figure 2. On the basis of the ASTM D6373, the mass change should be less than 1% during the RTFO aging procedure for asphalt binders. The mass of four asphalt residues decreased during the short-term aging procedure. The mass of CSS-1H and CRS-2TR residues decreased by more than 1%, which may have been because of the evaporation of surfactant in the emulsified asphalt.

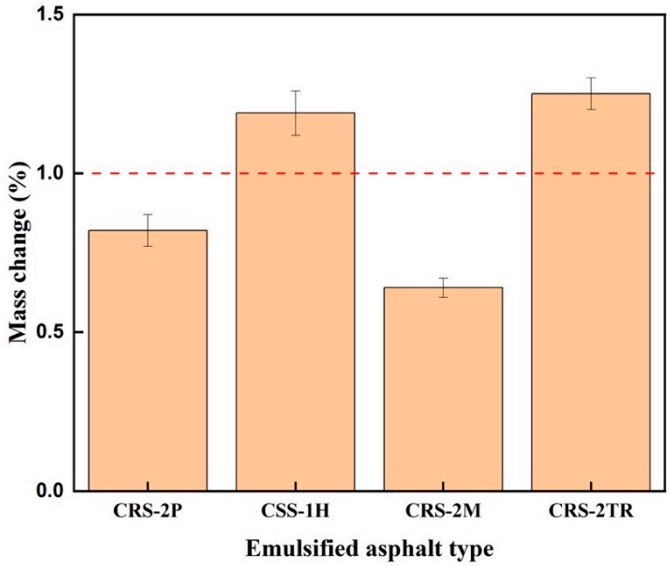

Figure 2. The mass change of emulsified asphalt residue during the rolling thin film oven (RTFO) test.

The FTIR test of four unaged residues during 3200–3550 cm^{-1} is displayed in Figure 3. No peak occurred during 3200–3550 cm^{-1} in the four emulsified asphalt residues acquired using the distillation process. The mass change of the emulsified asphalt binder during the RTFO process was not caused by the evaporation of water. The mass change only represented the components change of emulsified asphalt binder residue.

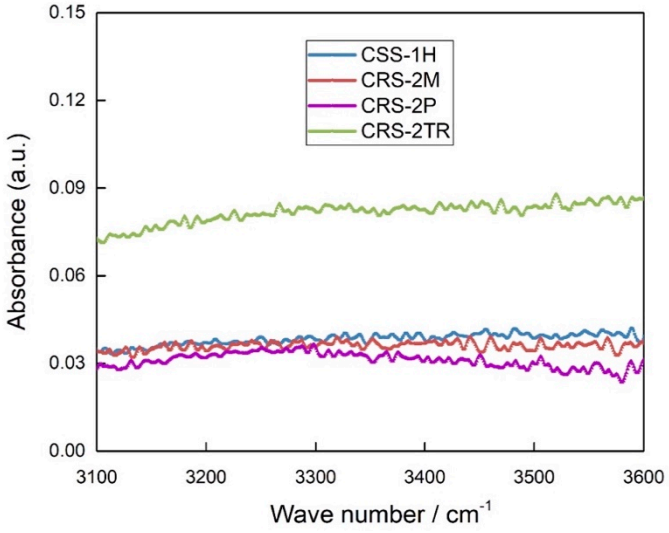

Figure 3. The FTIR test of four unaged residues during 3200–3550 cm^{-1}.

4.3. DSR Test

4.3.1. The Master Curve of |G*| Based on the DSR Test

Six different frequency sweeps under different test temperatures were applied to four types of emulsified asphalt residues. The master curve of |G*| was generated with a nonlinear regression method [52].

The master curve of the |G*| of four unaged emulsified asphalt residues is displayed in Figure 4. The property of asphalt binder at high reduced frequency could reflect the low-temperature properties. The modulus of the residue was enhanced when the temperature decreased, thus increasing the |G*|. The |G*| of CRS-2TR, CRS-2M, CRS-2P, and CSS-1H increased gradually. The |G*| differences between the CRS-2TR, CRS-2M, and CRS-2P were minimal when the reduced frequency was high. The maximum |G*| of CSS-1H was about five times higher than the maximum |G*| of CRS-2TR.

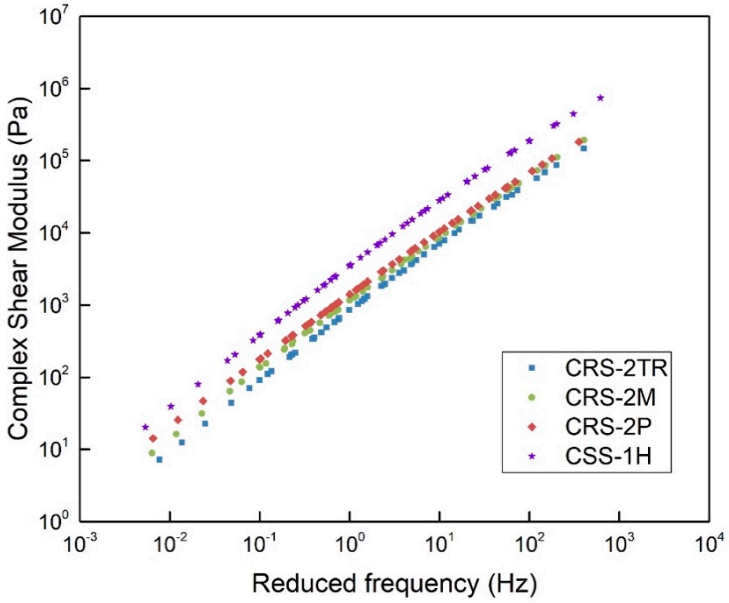

Figure 4. The master curve of |G*| of four unaged emulsified asphalt residues.

The master curve of the |G*| of four RTFO-aged emulsified asphalt residues are displayed in Figure 5. The |G*| of CRS-2TR, CRS-2M, and CRS-2P almost had no differences when the reduced frequency was high. The |G*| of CSS-1H was the highest among all residues. The |G*| of CSS-1H was two times larger at the low reduced frequency conditions and four times larger at the high reduced frequency conditions when compared with the other three emulsified asphalts. By comparing the |G*| of the test results in Figures 4 and 5, we found that the |G*| was increased after RTFO aging. The aging procedure oxidized the light component of the asphalt and increased the |G*|.

The master curve of the |G*| of the four PAV-aged emulsified asphalt residues are displayed in Figure 6. The |G*| of CRS-2P, CRS-2TR, CRS-2M, and CSS-1H increased gradually. The differences between the |G*| of different emulsified asphalt residues was increased after the PAV aging. The |G*| of CRS-2TR was similar to the |G*| of CRS-2M when the reduced frequency was low, and the |G*| of CRS-2P was similar to the |G*| of CRS-2TR when the reduced frequency was high. This may be because of the existence of 5% tire rubber in CRS-2TR. The |G*| of CSS-1H was four times larger than the |G*| of CRS-2P.

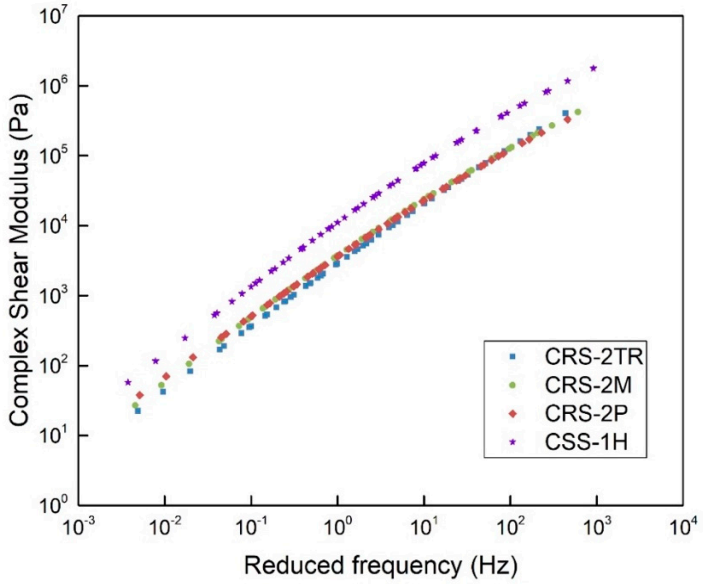

Figure 5. The master curve of |G*| of the four RTFO-aged emulsified asphalt residues.

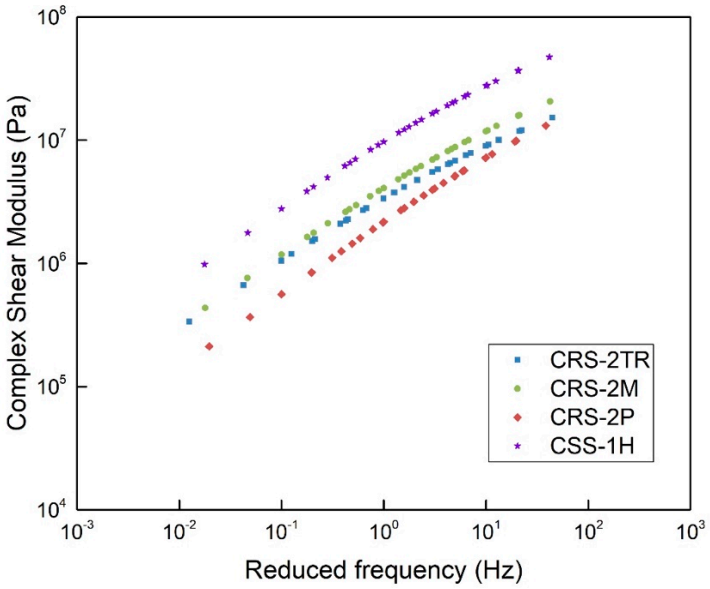

Figure 6. The master curve of |G*| of the four pressure aging vessel (PAV)-aged emulsified asphalt residues.

4.3.2. The Rutting Parameter (|G*|/sinδ) and the Fatigue Parameter (|G*|·sinδ)

The (|G*|/sinδ) of unaged emulsified asphalt under 10 rad/s angular frequency are displayed in Figure 7. The (|G*|/sinδ) of residues reduced when the test temperature was raised. The rutting parameter of the CSS-1H was remarkably higher than that of other emulsified asphalts. The CSS-1H passed the standard restriction (higher than 1.0 kPa) at 70 °C. The CRS-2P met the standard at 64 °C. The two emulsified asphalts, CRS-2M and CRS-2TR, fulfilled the criteria at 58 °C.

The rutting parameter of RTFO-aged emulsified asphalts under 10 rad/s angular frequency is displayed in Figure 8. The rutting parameter of the RTFO-aged binder had a trend similar to the unaged binder. The critical temperatures for the RTFO-aged samples of CSS-1H, CRS-2P, and CRS-2TR were the same as the unaged samples. The rutting parameter of RTFO-aged CRS-2M was higher than 2.2 kPa, even at 64 °C. The CRS-2M had better rutting resistance than CRS-2TR under the RTFO aging condition, which may have been because of the lower rubber content in CRS-2M.

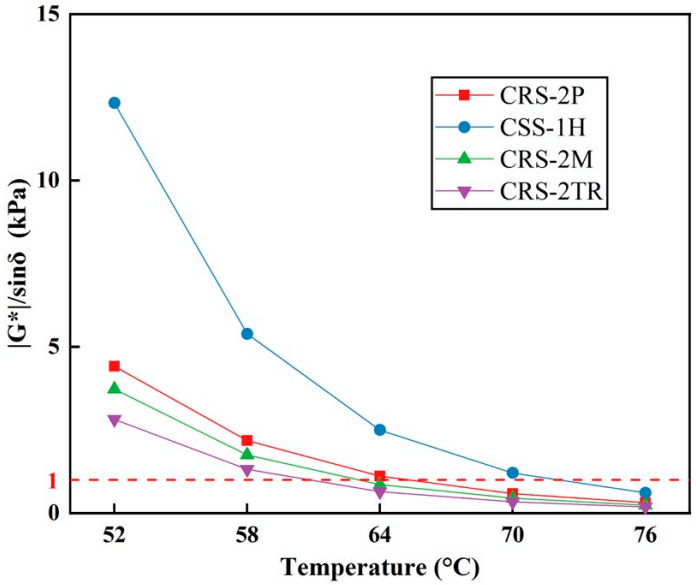

Figure 7. |G*|/sinδ of unaged emulsified asphalt residues.

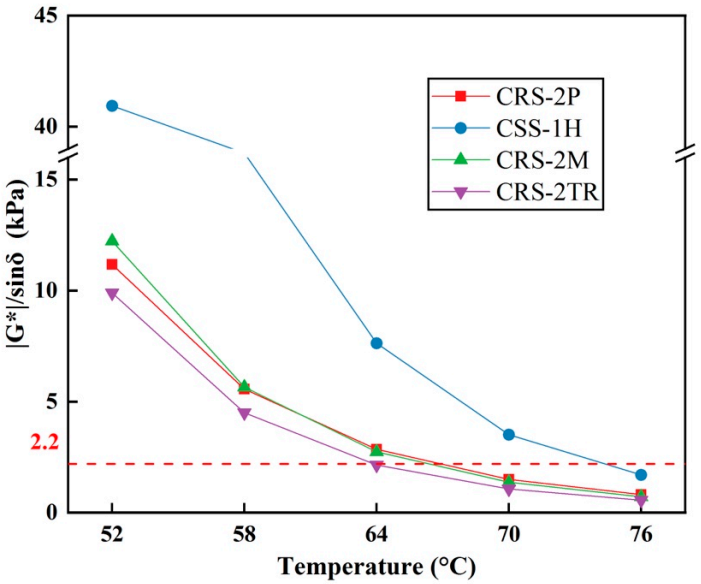

Figure 8. |G*|/sinδ of RTFO-aged emulsified asphalt residues.

On the basis of the DSR test, we found that the high-temperature performance grade of the CSS-1H (70 °C) was the highest, followed by CRS-2P (64 °C). The high-temperature properties of CRS-2M and CRS-2TR were the lowest (58 °C). The CSS-1H is formulated with harder base asphalt (low penetration), thus having better high-temperature properties. The original asphalt binder used for asphalt emulsification should be considered in quantifying the property of emulsified asphalt binders.

The |G*|·sinδ of PAV-aged emulsified asphalts are presented in Figure 9. CRS-2P and CRS-2TR still met the standard criteria (|G*|·sinδ lower than 5000 kPa) at 13 °C, which corresponded to a low-temperature performance grade lower than −40 °C. For CSS-1H, the |G*|·sinδ met the criteria at the temperature of 25 °C, which corresponded to a low-temperature performance grade of −28 °C. The CRS-2M met the requirements at a temperature of 16 °C, which corresponded to the low-temperature performance grade of −34 °C. Limited results could be observed on the low-temperature property of emulsified asphalt residues using the DSR test. The ABCD test was adopted to evaluate the low-temperature characteristics of the residues.

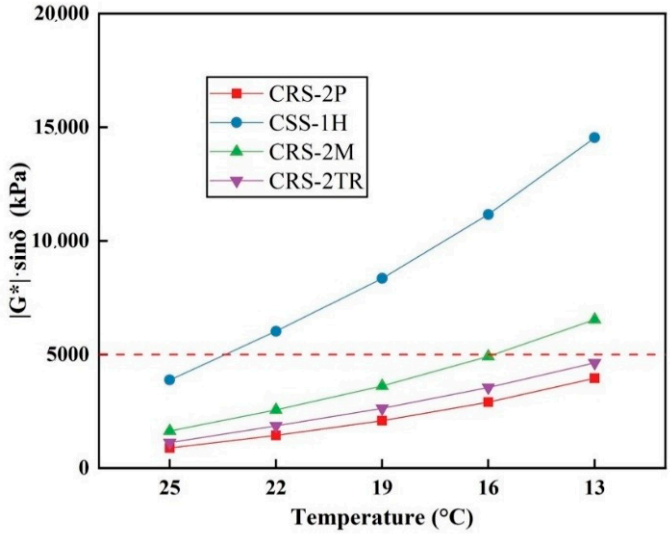

Figure 9. |G*|•sinδ of PAV-aged emulsified asphalt residues.

4.4. ABCD Test

The low-temperature properties of residues were assessed with the ABCD test. The thermal cracking temperature can be determined directly on the basis of the test. The fracture stress and the PG grade by ABCD can be calculated on the basis of Equations (1) and (2). The ABCD test results are displayed in Figure 10. According to the ABCD test, CRS-2M and CRS-2TR had higher strain jump and fracture stress than CRS-2P and CSS-1H. The crack temperature of the CRS-2M and CRS-2TR was lower, and the asphalt was more brittle at a lower temperature, thus having higher fracture stress. The temperature had a remarkable effect on the stress in the asphalt binder at low temperatures. The CRS-2P had a lower crack temperature than the CSS-1H, but the fracture stress of the CRS-2P was lower. Polymer modification could improve the stress relaxation ability of asphalt at low temperatures. On the basis of the ABCD test, we found that the CRS-2M and CRS-2TR emulsified asphalt binder residues had better low-temperature properties than other emulsified residues. The low-temperature characteristics of the emulsified asphalt were improved after adding rubber, and the improvement effect enhanced as the rubber content increased.

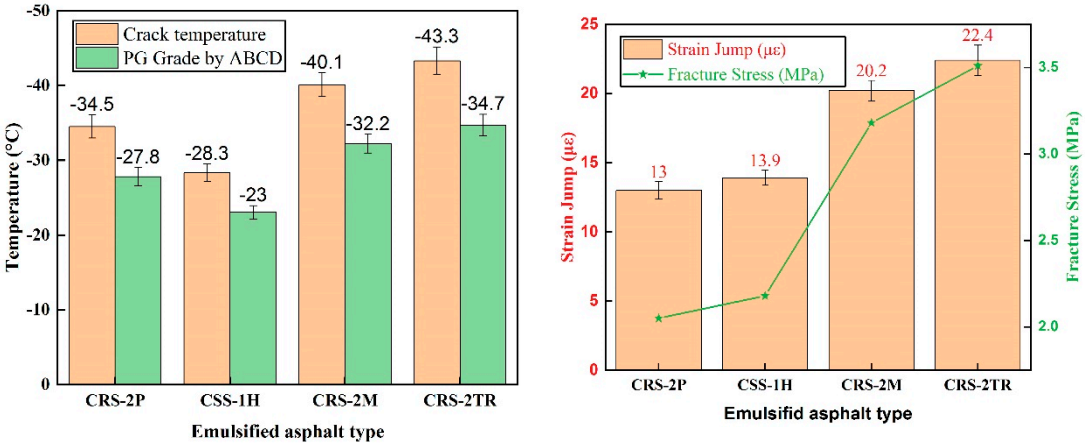

(**a**) Temperature (**b**) Stress and strain

Figure 10. The asphalt binder cracking device (ABCD) test results of different emulsified asphalt binder residues.

The performance-grade temperature for the four different emulsified asphalts is displayed in Table 3. CSS-1H had the best high-temperature property but had the worst low-temperature property. For CRS-2P, the high-temperature property was weaker and the low-temperature property was improved compared with CSS-1H. The high-temperature performance of the CRS-2M and CRS-2TR had the same high-temperature grade, but the low-temperature property of the CRS-2TR was better. Rubber addition could enhance the low-temperature characteristics of emulsified asphalt residue. The test samples are based on limited test samples, and more samples are needed in order to verify the conclusion. Furthermore, the influence of the original asphalt binder used to produce the emulsified asphalt binder should also be considered.

Table 3. The performance grade of different emulsified asphalts.

Emulsified Asphalt Type	High-Temperature (°C) DSR	Low-Temperature (°C) ABCD
CRS-2P	64	−27.8
CSS-1H	70	−23.0
CRS-2M	58	−32.2
CRS-2TR	58	−34.7

4.5. Fourier Transform Infrared (FTIR) Test

The change of chemical bonds in residues under different aging conditions were quantified with the FTIR test. The FTIR test results of different emulsified asphalt residues under different aging conditions is displayed in Figure 11. The band near 1000 cm^{-1} (S=O) and 1700 cm^{-1} (C=O) were enlarged to check the differences between different aging conditions. For CSS-1H, the S=O band had no differences between the control and short-term aged binders, and the area of S=O band after PAV aging increased dramatically. The C=O band area increased slightly after short-term aging and improved significantly after long-term aging (Figure 11a). For CRS-2P, the S=O band and the C=O band increased after RTFO and PAV aging (Figure 11b). For CRS-2M, the S=O band of the unaged binder was slightly higher than RTFO-aged binder, and the area of S=O band after PAV aging increased dramatically. The C=O band area increased slightly after short-term aging and improved significantly after long-term aging (Figure 11c). For CRS-2TR, the S=O band increased dramatically after PAV aging. The C=O band area increased slightly after short-term aging and improved significantly after long-term aging (Figure 11d).

In order to quantitatively evaluate the influence of aging on the emulsified asphalt residue, we calculated the band area of C=O and S=O under different aging conditions on the basis of the upper limit and lower limit and the baseline [53]. The spectrum area calculation results for the C=O band are shown in Figure 12. The C=O band area increased with the aging degree for all emulsified asphalt binder residues. The C=O band area of CRS-2P was the highest in four emulsified asphalt binders. The C=O band area of CRS-2TR was the lowest in four emulsified asphalt binders. The area increases for CSS-1H was lowest after the PAV aging. According to the DSR test result, the |G*| of the CSS-1H was the highest, and the stiffness of the CSS-1H was higher. The influence of long-term aging was the least.

The spectrum area calculation results for the S=O band are presented in Figure 13. The S=O band area was lower than the C=O band area. For CRS-2P, the S=O band area of RTFO-aged samples was higher than that of unaged and PAV aged samples. For CRS-2TR, the S=O band area of RTFO-aged samples was lower than that of unaged and long-term aged samples. The differences between the unaged and short-term aged asphalts were minimal for the CSS-1H and the CRS-2M. The S=O band area did not match to the aging condition of CRS-2P residue.

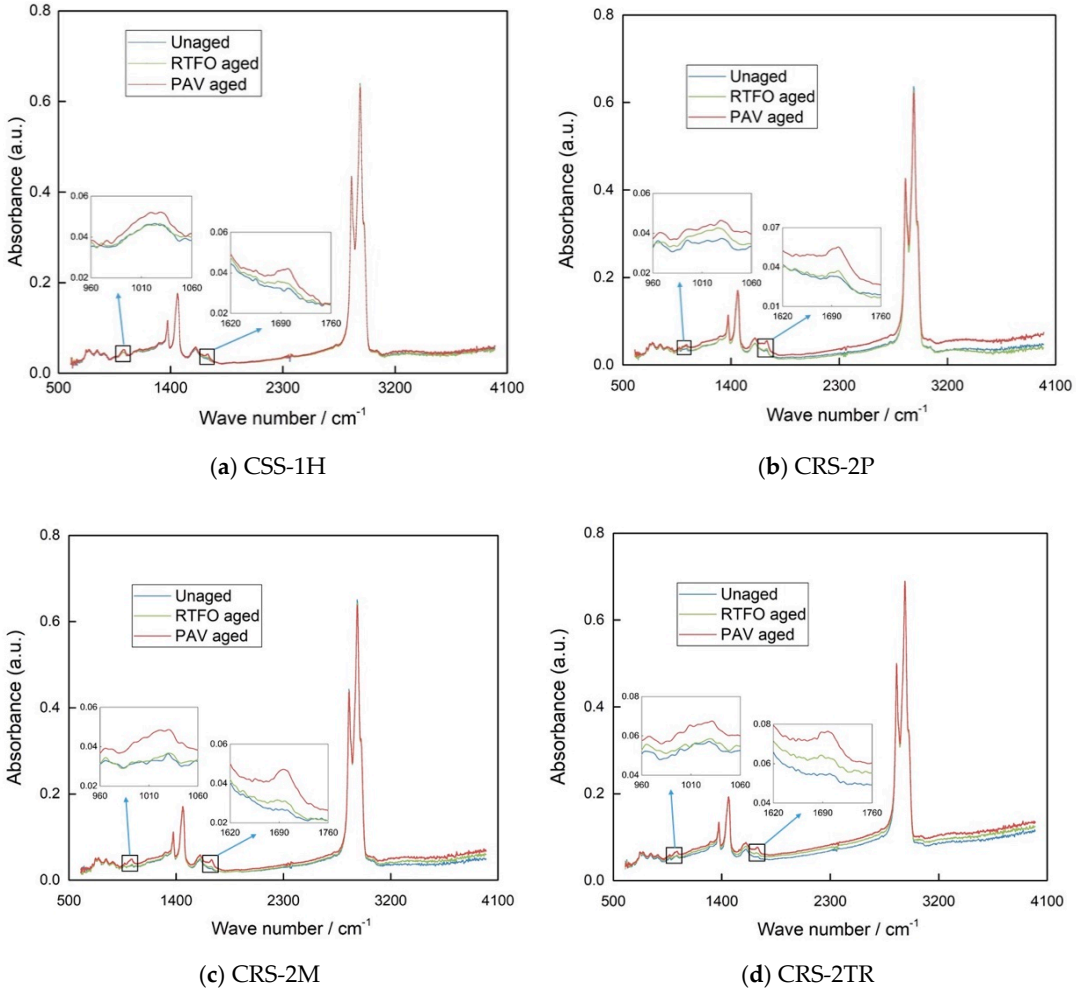

Figure 11. The FTIR test results of different emulsified asphalt residues under different aging conditions.

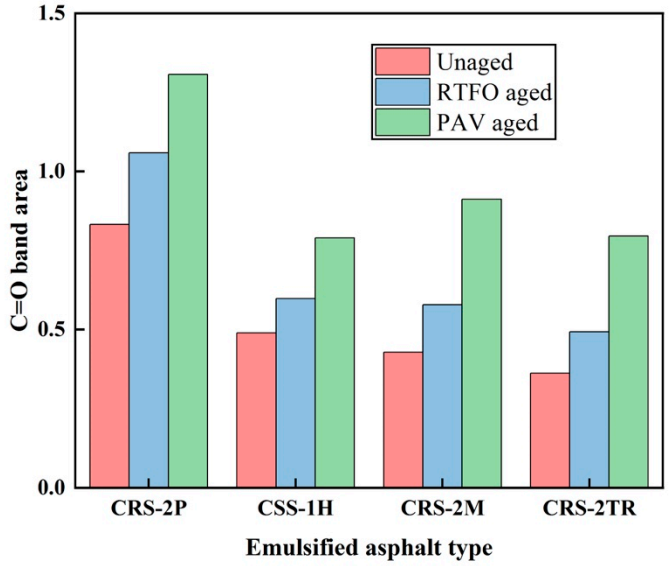

Figure 12. Spectrum area of C=O band under different aging conditions.

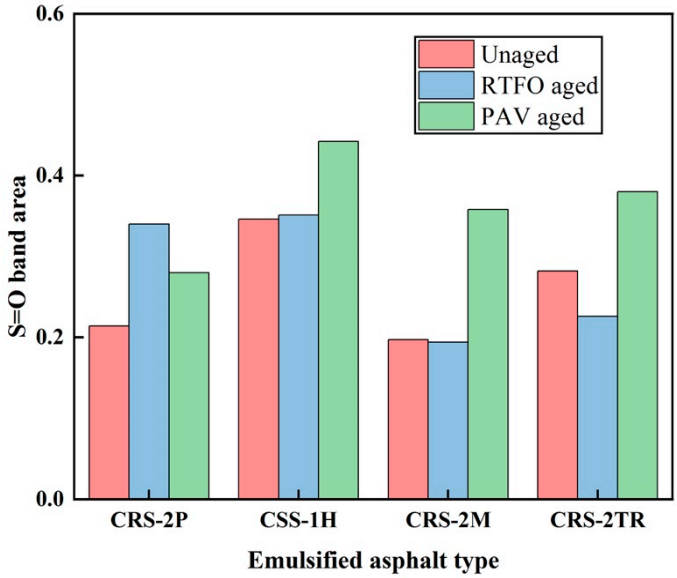

Figure 13. Spectrum area of S=O band under different aging conditions.

5. Conclusions

In this study, we evaluated four emulsified asphalt binders applied in wet-freeze regions. The property of rubber-modified emulsified asphalt was compared with that of polymer-modified asphalt and conventional emulsified asphalt. The distillation residue was RTFO-aged and PAV-aged in the lab. The DSR, ABCD, and FTIR tests were adopted to investigate the property of emulsified asphalt residue.

The main conclusions are presented below, on the basis of the test results:

1. The evaporation method was less effective than the distillation method in removing water from residue.
2. The mass change during the RTFO process only represented the component change of emulsified asphalt binder residue.
3. The high-temperature property of the CSS-1H was the best, and the high-temperature properties of the two emulsified asphalts with rubber were the worst. The original asphalt binder used to produce emulsified asphalt had a remarkable influence on the characteristics of emulsified asphalt.
4. Polymer modification could enhance the low-temperature property of the emulsified asphalt. The low-temperature properties of CRS-2M and CRS-2TR residue were improved. The rubber modification enhanced the low-temperature characteristics of the emulsified asphalt binder, and the improvement effect enhanced as the rubber content increased.
5. The C=O band was more sensitive to the aging condition of the residue than S=O, which can be used as an index to quantify the aging condition of the residue.

Author Contributions: Conceptualization, D.G. and Z.Y.; methodology, D.G. and S.C.; validation, D.G., X.Z., and D.J.; formal analysis, D.G.; investigation, D.G.; resources, Z.Y.; data curation, D.G.; writing—original draft preparation, D.G.; writing—review and editing, D.G., X.Z., S.C., D.J., and Z.Y.; visualization, D.G.; supervision, Z.Y.; project administration, Z.Y.; funding acquisition, Z.Y. All authors have read and agreed to the published version of the manuscript.

Funding: This study is sponsored and partially funded by the Michigan Department of Environment, Great Lakes, and Energy (EGLE) of the United States.

Acknowledgments: We appreciate the assistance of Muskegon County Road Commission in Michigan during this project.

Conflicts of Interest: The authors declare no conflict of interest.

References

1. Marasteanu, M.O.; Clyne, T.R. Rheological characterization of asphalt emulsions residues. *J. Mater. Civ. Eng.* **2006**, *18*, 398–407. [CrossRef]
2. Pang, J.Y.; Du, S.J.; Chang, R.T.; Pei, Q.; Cui, D.X. Effect of emulsifier content on the rheological properties of asphalt emulsion residues. *J. Appl. Polym. Sci.* **2015**, *132*, 7. [CrossRef]
3. Takamura, K. Characterization of emulsion based warm mix binder. *Road Mater. Pavement Des.* **2008**, *9*, 87–102. [CrossRef]
4. Yuliestyan, A.; Garcia-Morales, M.; Moreno, E.; Carrera, V.; Partal, P. Assessment of modified lignin cationic emulsifier for bitumen emulsions used in road paving. *Mater. Des.* **2017**, *131*, 242–251. [CrossRef]
5. Ilias, M.; Adams, J.; Castorena, C.; Kim, Y.R. Performance-related specifications for asphalt emulsions used in microsurfacing treatments. *Transp. Res. Record* **2017**, *2632*, 1–13. [CrossRef]
6. Hanz, A.J.; Johannes, P.; Bahia, H.U. Development of emulsion residue testing framework for improved chip seal performance. *Transp. Res. Rec. J. Transp. Res. Board* **2012**, *2293*, 106–113. [CrossRef]
7. Khadivar, A.; Kavussi, A. Rheological characteristics of SBR and NR polymer modified bitumen emulsions at average pavement temperatures. *Constr. Build. Mater.* **2013**, *47*, 1099–1105. [CrossRef]
8. Abedini, M.; Hassani, A.; Kaymanesh, M.R.; Yousefi, A.A. The rheological properties of a bitumen emulsion modified with two types of SBR latex. *Pet. Sci. Technol.* **2016**, *34*, 1589–1594. [CrossRef]
9. Abedini, M.; Hassani, A.; Kaymanesh, M.R.; Yousefi, A.A.; Abedini, H. Multiple stress creep and recovery behavior of SBR-modified bitumen emulsions. *J. Test. Eval.* **2020**, *48*. [CrossRef]
10. Ferdous, W.; Manalo, A.; Wong, H.S.; Abousnina, R.; AlAjarmeh, O.S.; Zhuge, Y.; Schubel, P. Optimal design for epoxy polymer concrete based on mechanical properties and durability aspects. *Constr. Build. Mater.* **2020**, *232*, 117229. [CrossRef]
11. Sarkar, M.T.A.; Rahman, M.N.; Elseifi, M.A.; Mayeux, C.; Cooper, S.B., III. Rheological and molecular characterizations of tire rubber modified asphalt emulsion. *Transp. Res. Record* **2020**. [CrossRef]
12. Forbes, A.; Haverkamp, R.G.; Robertson, T.; Bryant, J.; Bearsley, S. Studies of the microstructure of polymer-modified bitumen emulsions using confocal laser scanning microscopy. *J. Microsc.* **2001**, *204*, 252–257. [CrossRef] [PubMed]
13. Cuadri, A.; Roman, C.; Garcia-Morales, M.; Guisado, F.; Moreno, E.; Partal, P. Formulation and processing of recycled-low-density-polyethylene-modified bitumen emulsions for reduced-temperature asphalt technologies. *Chem. Eng. Sci.* **2016**, *156*, 197–205. [CrossRef]
14. Chen, X.; Wang, H.N.; Wang, Q.H.; Yang, X.; You, Z.P. Optimization of laboratory preparation of the emulsified bioasphalt with two emulsifiers. *J. Test. Eval.* **2018**, *46*, 1343–1354. [CrossRef]
15. Sheng, X.; Wang, M.; Xu, T.; Chen, J. Preparation, properties and modification mechanism of polyurethane modified emulsified asphalt. *Constr. Build. Mater.* **2018**, *189*, 375–383. [CrossRef]
16. Taha, R.; Hassan, H.; Al-Rawas, A.; Yaghi, B.; Al-Futaisi, A.; Jamrah, A.; Al-Suleimani, Y. Use of tank bottom sludge to construct and upgrade unpaved roads. *Transp. Res. Record* **2007**, 208–214. [CrossRef]
17. Carrera, V.; Cuadri, A.; García-Morales, M.; Partal, P. The development of polyurethane modified bitumen emulsions for cold mix applications. *Mater. Struct.* **2015**, *48*, 3407–3414. [CrossRef]
18. Li, R.; Leng, Z.; Zhang, Y.; Ma, X. Preparation and characterization of waterborne epoxy modified bitumen emulsion as a potential high-performance cold binder. *J. Clean. Prod.* **2019**, *235*, 1265–1275. [CrossRef]
19. Gutiérrez Klinsky, L.M.; Motta, R.; Bariani Bernucci, L.L. Cold recycled asphalt mixture using 100% RAP with emulsified asphalt-recycling agent as a new pavement base course. *Adv. Mater. Sci. Eng.* **2020**, *2020*. [CrossRef]
20. Yang, X.; You, Z.; Perram, D.; Hand, D.; Ahmed, Z.; Wei, W.; Luo, S. Emission analysis of recycled tire rubber modified asphalt in hot and warm mix conditions. *J. Hazard. Mater.* **2019**, *365*, 942–951. [CrossRef]
21. Ling, C.; Moraes, R.; Swiertz, D.; Bahia, H. Measuring the influence of aggregate coating on the workability and moisture susceptibility of cold-mix asphalt. *Transp. Res. Record* **2013**, *2372*, 46–52. [CrossRef]
22. Abd El-Rahman, A.M.M.; El-Shafie, M.; Abo-Shanab, Z.L.; El-Kholy, S.A. Modifying asphalt emulsion with different types of polymers for surface treatment applications. *Pet. Sci. Technol.* **2017**, *35*, 1473–1480. [CrossRef]
23. Ma, T.; Wang, H.; Zhao, Y.; Huang, X. Laboratory investigation on residual strength of reclaimed asphalt mixture for cold mix recycling. *Int. J. Pavement Res. Technol.* **2015**, *8*. [CrossRef]

24. Cardone, F.; Virgili, A.; Graziani, A. Evaluation of bonding between reclaimed asphalt aggregate and bitumen emulsion composites. *Constr. Build. Mater.* **2018**, *184*, 565–574. [CrossRef]
25. Li, Y.; Lyv, Y.; Fan, L.; Zhang, Y. Effects of cement and emulsified asphalt on properties of mastics and 100% cold recycled asphalt mixtures. *Materials* **2019**, *12*, 754. [CrossRef] [PubMed]
26. Du, S. Interaction mechanism of cement and asphalt emulsion in asphalt emulsion mixtures. *Mater. Struct.* **2014**, *47*, 1149–1159. [CrossRef]
27. Chavez-Valencia, L.; Alonso, E.; Manzano, A.; Perez, J.; Contreras, M.; Signoret, C. Improving the compressive strengths of cold-mix asphalt using asphalt emulsion modified by polyvinyl acetate. *Constr. Build. Mater.* **2007**, *21*, 583–589. [CrossRef]
28. Jiang, J.; Ni, F.; Zheng, J.; Han, Y.; Zhao, X. Improving the high-temperature performance of cold recycled mixtures by polymer-modified asphalt emulsion. *Int. J. Pavement Eng.* **2020**, *21*, 41–48. [CrossRef]
29. Hoyt, D.; Martin, A.E.; Shuler, S. Surface performance-grading system to grade chip seal emulsion residues. *Transp. Res. Rec. J. Transp. Res. Board* **2010**, *2150*, 63–69. [CrossRef]
30. ASTM. Standard practice for recovering residue from emulsified asphalt using low temperature evaporative technique. In *ASTM D7497*; ASTM International: West Conshohocken, PA, USA, 2016.
31. Malladi, H.; Asnake, M.; LaCroix, A.; Castorena, C. Low-temperature vacuum drying procedure for rapid asphalt emulsion residue recovery. *Transp. Res. Record* **2018**, *2672*, 256–265. [CrossRef]
32. Farrar, M.J.; Salmans, S.L.; Planche, J.P. Recovery and laboratory testing of asphalt emulsion residue application of simple aging test and 4-mm dynamic shear rheometer test. *Transp. Res. Record* **2013**, 69–75. [CrossRef]
33. Boysen, R.B.; Farrar, M.J.; Planche, J.-P. Quantification of water in asphalt by Karl Fischer titration and its application to emulsion recovery. *Transp. Res. Record* **2014**, *2444*, 97–101. [CrossRef]
34. ASTM. Standard test method for residue by evaporation of emulsified asphalt. In *ASTM D6934*; ASTM International: West Conshohocken, PA, USA, 2016.
35. ASTM. Standard test method for distillation of emulsified asphalt. In *ASTM D6997*; ASTM International: West Conshohocken, PA, USA, 2012.
36. Prapaitrakul, N.; Han, R.; Jin, X.; Martin, A.E.; Glover, C.J. Comparative study on recovered binder properties using three asphalt emulsion recovery methods. *J. Test. Eval.* **2010**, *38*, 653–659.
37. Salomon, D.; Thompson, M.; Dur, G.; Gueit, C.; Deneuvillers, C.; Robert, M.; Lebon, A.; Sa, C. Comparison of rheological properties for recovered residue from emulsified asphalt obtained by three recovery procedures. In Proceedings of the 2008 International Symposium of Asphalt Emulsion Technology (ISAET), Washington, DC, USA, 26 September 2008.
38. Sun, Y.; Yue, J.-C.; Wang, R.-R.; Li, R.-X.; Wang, D.-C. Investigation of the effects of evaporation methods on the high-temperature rheological and fatigue performances of emulsified asphalt residues. *Adv. Mater. Sci. Eng.* **2020**, *2020*. [CrossRef]
39. Islam, R.M.; Ashani, S.S.; Wasiuddin, N.M. Effects of curing time, temperature, and vacuum pressure on asphalt emulsion residue recovered by vacuum drying method. *J. Test. Eval.* **2015**, *43*, 1134–1145. [CrossRef]
40. ASTM. Standard test method for effect of heat and air on a moving film of asphalt (rolling thin-film oven test). In *ASTM D2872*; ASTM International: West Conshohocken, PA, USA, 2012.
41. ASTM. Standard practice for accelerated aging of asphalt binder using a pressurized aging vessel (pav). In *ASTM D6521*; ASTM International: West Conshohocken, PA, USA, 2018.
42. Ge, D.; Yan, K.; Ye, F.; Zhao, X. The laboratory performance of asphalt mixture with Amorphous poly alpha olefins (APAO) modified asphalt binder. *Constr. Build. Mater.* **2018**, *188*, 676–684. [CrossRef]
43. Zhang, R.; You, Z.; Wang, H.; Ye, M.; Yap, Y.K.; Si, C. The impact of bio-oil as rejuvenator for aged asphalt binder. *Constr. Build. Mater.* **2019**, *196*, 134–143. [CrossRef]
44. Yao, H.; Dai, Q.; You, Z.; Ye, M.; Yap, Y.K. Rheological properties, low-temperature cracking resistance, and optical performance of exfoliated graphite nanoplatelets modified asphalt binder. *Constr. Build. Mater.* **2016**, *113*, 988–996. [CrossRef]
45. You, Z.; Mills-Beale, J.; Fini, E.; Goh, S.W.; Colbert, B. Evaluation of low-temperature binder properties of warm-mix asphalt, extracted and recovered RAP and RAS, and bioasphalt. *J. Mater. Civ. Eng.* **2011**, *23*, 1569–1574. [CrossRef]
46. Kim, S.S. *Development of an Asphalt Binder Cracking Device*; IDEA Program, Transportation Research Board: Washington, DC, USA, 2007.

47. Ge, D.; You, Z.; Chen, S.; You, L. Using DSR and FTIR to evaluate asphalt binder extracted and recovered from asphalt mixtures. In Proceedings of the Congress on Technical Advancement 2017, Duluth, MI, USA, 10–13 September 2017; pp. 89–105.
48. Yao, H.; You, Z.; Li, L.; Lee, C.H.; Wingard, D.; Yap, Y.K.; Shi, X.; Goh, S.W. Rheological properties and chemical bonding of asphalt modified with nanosilica. *J. Mater. Civ. Eng.* **2013**, *25*, 1619–1630. [CrossRef]
49. Khotbehsara, M.M.; Manalo, A.; Aravinthan, T.; Reddy, K.R.; Ferdous, W.; Wong, H.; Nazari, A. Effect of elevated in-service temperature on the mechanical properties and microstructure of particulate-filled epoxy polymers. *Polym. Degrad. Stab.* **2019**, *170*, 108994. [CrossRef]
50. Yang, X.; You, Z.; Mills-Beale, J. Asphalt binders blended with a high percentage of biobinders: Aging mechanism using FTIR and rheology. *J. Mater. Civ. Eng.* **2015**, *27*, 04014157. [CrossRef]
51. Ge, D.; Chen, S.; You, Z.; Yang, X.; Yao, H.; Ye, M.; Yap, Y.K. Correlation of DSR results and FTIR's carbonyl and sulfoxide indexes: Effect of aging temperature on asphalt rheology. *J. Mater. Civ. Eng.* **2019**, *31*, 04019115. [CrossRef]
52. Yang, X.; You, Z. New predictive equations for dynamic modulus and phase angle using a nonlinear least-squares regression model. *J. Mater. Civ. Eng.* **2014**, *27*, 04014131. [CrossRef]
53. Ge, D.; You, Z.; Chen, S.; Liu, C.; Gao, J.; Lv, S. The performance of asphalt binder with trichloroethylene: Improving the efficiency of using reclaimed asphalt pavement. *J. Clean. Prod.* **2019**, *232*, 205–212. [CrossRef]